

A signature of the donor star in the extra-galactic X-ray binary LMC X-2

R. Cornelisse^{1,2*}, D. Steeghs^{3,4}, J. Casares¹, P.A. Charles^{5,2}, I.C. Shih^{6,2},
R.I. Hynes⁷, K. O’Brien⁸

¹*Instituto de Astrofísica de Canarias, Via Lactea, La Laguna E-38200, Santa Cruz de Tenerife, Spain*

²*School of Physics and Astronomy, University of Southampton, Highfield, Southampton SO17 1BJ, UK*

³*Harvard-Smithsonian Center for Astrophysics, 60 Garden Street, Cambridge, MA 02138, USA*

⁴*Department of Physics, University of Warwick, Coventry, CV4 7AL, UK*

⁵*South Africa Astronomical Observatory, P.O.Box 9.Observatory 7935, South Africa*

⁶*Department of Physics & Astronomy, Michigan State University, East Lansing, MI 48824, USA*

⁷*Department of Physics and Astronomy, 202 Nicholson Hall, Louisiana State University, Baton Rouge, LA 70803, USA*

⁸*European Southern Observatory, Casilla 19001, Santiago 19, Chile*

Accepted Received ; in original form

ABSTRACT

Two nights of phase-resolved medium resolution VLT spectroscopy of the extra-galactic low mass X-ray binary LMC X-2 have revealed a 0.32 ± 0.02 day spectroscopic period in the radial velocity curve of the He II $\lambda 4686$ emission line that we interpret as the orbital period. However, similar to previous findings, this radial velocity curve shows a longer term variation that is most likely due to the presence of a precessing accretion disk in LMC X-2. This is strengthened by He II $\lambda 4686$ Doppler maps that show a bright spot that is moving from night to night. Furthermore, we detect narrow emission lines in the Bowen region of LMC X-2, with a velocity of $K_{\text{em}} = 351 \pm 28$ km s^{-1} , that we tentatively interpret as coming from the irradiated side of the donor star. Since K_{em} must be smaller than K_2 , this leads to the first upper-limit on the mass function of LMC X-2 of $f(M_1) \geq 0.86 M_{\odot}$ (95% confidence), and the first constraints on its system parameters.

Key words: accretion, accretion disks – stars:individual (LMC X-2) – X-rays:binaries.

1 INTRODUCTION

Low mass X-ray binaries (LMXBs) are compact binaries where the primary is a compact object and the secondary a low mass star ($\leq 1 M_{\odot}$). The secondary is transferring mass via Roche-lobe overflow, forming an accretion disk around the compact object that gives rise to the observed X-rays. By far, most of the persistently bright LMXBs are neutron star systems that can be divided into two groups, the Z-sources and Atoll sources (Hasinger & van der Klis 1989). Z-sources are usually the brightest LMXBs in X-rays (they are thought to have mass accretion rates that reach the Eddington limit) and trace a Z-like shape in their X-ray colour-colour diagrams. Atoll sources on the other hand have lower accretion rates ($\simeq 1$ -2 orders of magnitude lower) and their colour-colour diagrams usually consists of fragmented ‘island-like’ regions. Apart from the difference in accretion

rates, the main physical difference between Z-sources and Atoll sources are thought to be the strength of the neutron star magnetic field and their evolutionary history (Hasinger & van der Klis 1989).

LMC X-2 is a persistent LMXB that shows the properties of a Z-source (Smale et al. 2003), and it is therefore thought to be a neutron star system that has an accretion rate around the Eddington limit. It is one of the most X-ray luminous LMXBs known ($L_X \simeq 10^{38}$ erg s^{-1}), but due to its extra-galactic nature (it is located in the Large Magellanic Cloud at a distance of $\simeq 48$ kpc), its X-ray flux is rather low. Its optical counterpart was identified by Pakull (1978) as a $B \sim 18.5$ blue star. Despite being X-ray luminous and having a known optical counterpart, thus far little is known about the system parameters of LMC X-2. Even the estimates for the orbital period range from 6.4 hrs (Motch et al. 1985) or 8.2 hrs (Callanan et al. 1990, Smale & Kuulkers 2000) up to 12 days by Crampton et al. (1990). To make things even

* E-mail: corneli@iac.es

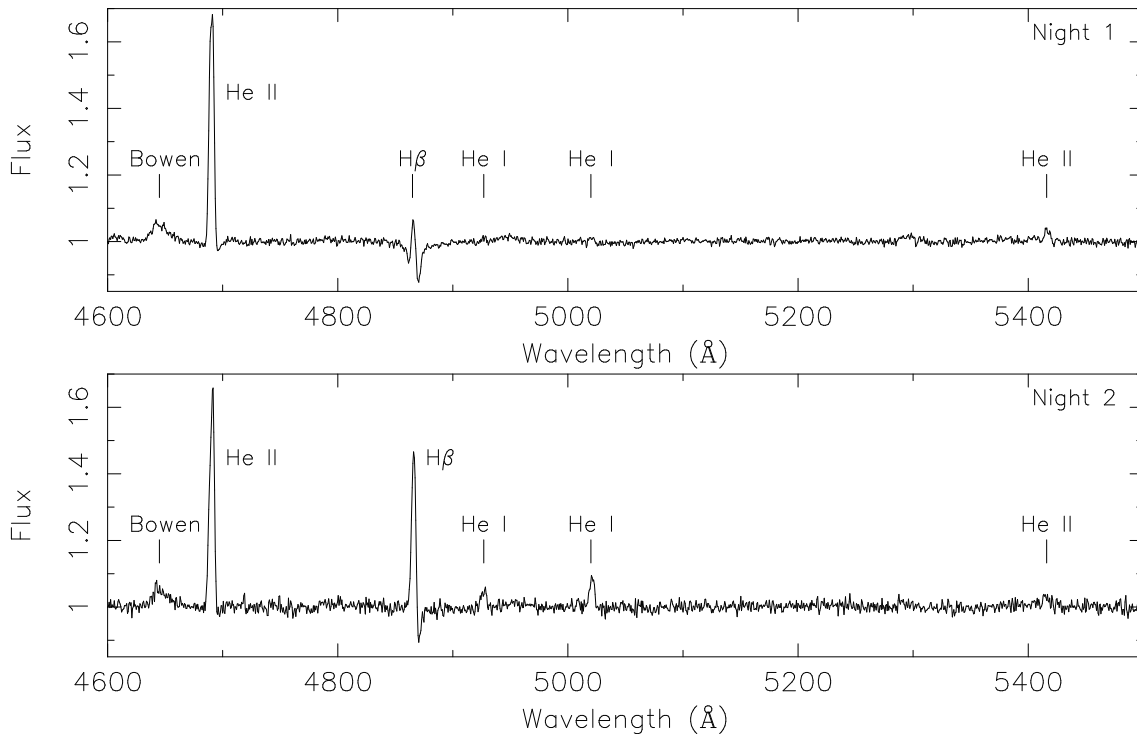


Figure 1. Average spectrum of LMC X-2 during the first observing night (top) and the second night (bottom).

more complicated, no periodic variability was detected in 6 years of MACHO data (Alcock et al. 2000).

In recent years Steeghs & Casares (2002) developed a new technique to detect a signature of the donor star in persistent LMXBs. Using phase-resolved spectroscopy they detected narrow emission lines in Sco X-1, especially in the Bowen blend (a blend of N III and C III lines between 4630-4650 Å), that were interpreted as coming from the irradiated side of the donor star. This discovery in Sco X-1 was followed by a survey of other LMXBs that are optically bright enough to also resolve these narrow components. Thus far these narrow emission lines have been detected in X 1822–371 (Casares et al. 2003), GX 339–4 (Hynes et al. 2003), V801 Ara and V926 Sco (Casares et al. 2006), GR Mus (Barnes et al. 2007), Aql X-1 and GX 9+9 (Cornelisse et al. 2007a,b), leading to constraints on their system parameters.

In this paper we apply the technique of Bowen fluorescence to LMC X-2. We will show that it is possible to detect a periodic signal in our spectroscopic dataset that we identify as the orbital period. Furthermore, similar to the other X-ray binaries thus far, the Bowen region shows the presence of narrow emission lines that we identify as coming from the irradiated side of the companion, giving the first ever constraints on the system parameters of LMC X-2.

2 OBSERVATIONS AND DATA REDUCTION

On November 21 and 22 2004 we obtained a total of 77 spectra of LMC X-2 with an integration time of 600 s each, using the FORS2 spectrograph attached to the VLT Unit 4 (Yepun Telescope) at Paranal Observatory (ESO). Each spectrum was taken with the 1400V volume-phased holo-

graphic grism using a slit width of $0.7''$, giving a wavelength coverage of $\lambda\lambda 4514\text{--}5815$ and a resolution of 70 km s^{-1} (FWHM). The seeing during the first night was between 0.4 and 0.7 arcsec, while on the second night it varied between 0.5 and 2.7 arcs. The slit was orientated at a position angle of 7° to include a comparison star in order to correct for slit losses. During daytime He, Ne, Hg and Cd arc lamp exposures were taken for the wavelength calibration scale. We de-biased and flat-fielded all the images and used optimal extraction techniques to maximise the signal-to-noise ratio of the extracted spectra (Horne 1986). We determined the pixel-to-wavelength scale using a 4th order polynomial fit to 20 reference lines giving a dispersion of $0.64 \text{ \AA pixel}^{-1}$ and rms scatter $<0.05 \text{ \AA}$. We also corrected for any velocity drifts due to instrumental flexure by cross-correlating the sky spectra. Finally, we divided all spectra of LMC X-2 by a corresponding low order spline-fit of the comparison star to get the final fluxed spectra. Since we did not observe a spectro-photometric standard star, we were not able to correct for instrumental response, and all spectra are therefore in relative fluxes.

3 DATA ANALYSIS

3.1 Spectral characteristics

We created average spectra for each individual night. Since we do not have a flux standard to derive an absolute flux for LMC X-2, we decided to normalise the continuum flux to one by dividing each average spectrum by a low order spline fit. In Fig. 1 we show the results. Both spectra are dominated by the very narrow high excitation He II $\lambda 4686$ emission line, while also Bowen emission is present in both spectra. How-

ever, compared to other X-ray binaries, such as Sco X-1, X 1822–371, V801 Ara and V926 Sco the Bowen emission is much weaker compared to He II in LMC X-2 (Steeeghs & Casares 2002, Casares et al. 2003, Casares et al. 2006). This might be due to the much lower metal abundances in the Large Magellanic Cloud (Motch & Pakull 1979). The most striking difference between the spectra is the dramatic change of $H\beta$ (see Fig. 1). During the first night (21 November) $H\beta$ is dominated by a weak emission feature superposed on a broad absorption feature, while in the second night (22 November) the emission feature has become almost as strong as He II $\lambda 4686$. Furthermore, also the He I $\lambda 4922/5016$ lines have become more prominent during the second night (although they might be present during the first night).

In order to quantify the change in the most prominent emission lines we estimated the equivalent widths and their line fluxes (in arbitrary units) for the two nights, and show them in Table 1. For $H\beta$ we decided to also include the absorption component, giving negative values for the first night. Table 1 shows that there is no change in equivalent width of He II and the Bowen region, and the line fluxes have dropped by $\simeq 40\%$ during the second night. On the other hand the $H\beta$ and He I lines have all increased significantly in both equivalent width and line flux. Unfortunately, due to the faintness of these lines (or the presence of an absorption feature), it is not possible to say if they have all changed by the same amount, but it is likely that the same process is responsible for this change in line intensity. Finally, in order to see if these changes could be related to a change in brightness we have also created a lightcurve of the continuum flux for LMC X-2. We have normalised the flux of the first night around unity, and show the result in Fig. 2. We note that during the second night the continuum flux was $\simeq 40\%$ lower compared to the first night, a similar fraction as was observed for the line fluxes of the He II lines and Bowen region, keeping their equivalent widths the same and suggesting a common origin.

3.2 Radial Velocities

We determined phase-resolved radial velocities by cross-correlating each spectrum with a Gaussian of width 150 km s^{-1} centered on the core of the He II $\lambda 4686$ line. Since the conditions during the second night were much worse, together with the fact that the source was $\simeq 40\%$ fainter, we have binned these spectra together in groups of three, and then determined the radial velocity. In Fig. 3 we show the results.

The first thing to note in Fig. 3 is that during both nights the radial velocity shows a sine-like variation, which we interpret as orbital motion of a region that is co-rotating with the binary, and perhaps is connected to the dynamical properties of the primary. However, during the second night it appears that either the semi-amplitude of the radial velocity or the off-set compared to the rest wavelength has increased. This last behaviour was noted by Crampton et al. (1990), who observed a long-term variation in the radial velocity of He II.

We searched the radial velocity curve for any periodic signal with a duration between 1 hr and 2 days using the Lomb-Scargle technique (Scargle 1982). Apart from the 24 hr alias due to the separation of our 2 observing nights, only

Table 1. LMC X-2 equivalent widths and spectral line fluxes.

| line | Night 1 EW (Å) | Flux | Night 2 EW (Å) | Flux |
|----------------------|-------------------|-----------------|-------------------|-----------------|
| He II $\lambda 4686$ | 3.20 ± 0.06 | 182.7 ± 0.9 | 3.07 ± 0.08 | 112.1 ± 1.2 |
| Bowen | 0.85 ± 0.06 | 35.6 ± 0.7 | 0.81 ± 0.08 | 23.6 ± 1.0 |
| He II $\lambda 5411$ | 0.19 ± 0.03 | 9.2 ± 0.8 | 0.22 ± 0.04 | 8.4 ± 0.9 |
| $H\beta$ | -0.70 ± 0.03 | -43.0 ± 0.9 | 1.59 ± 0.06 | 49.9 ± 1.1 |
| He I $\lambda 4922$ | 0.04 ± 0.03 | 3.8 ± 1.1 | 0.26 ± 0.04 | 15.1 ± 1.4 |
| He I $\lambda 5016$ | 0.03 ± 0.03 | 3.3 ± 1.1 | 0.44 ± 0.04 | 27.5 ± 1.4 |

two significant peaks with comparable strength were present in the power spectrum; one peak is at a period of 0.32 ± 0.02 days and another at 0.45 ± 0.05 day. Interestingly, the 0.32 day period is similar to the photometric period detected by Callanan et al. (1990), suggesting that this is the orbital period. Although we cannot exclude the possibility that the 0.45 day period is real (but see Sect. 3.3), we tentatively interpret the 0.32 day period as the orbital period and use it in the rest of this paper. Fitting a sine curve with a period of 0.32 day to the radial velocity curve gives a phase zero at HJD $2,453,330.41 \pm 0.03$, an off-set of $344 \pm 11 \text{ km s}^{-1}$, and the semi-amplitude of our sine fit is $41 \pm 4 \text{ km s}^{-1}$. Note that we did not attempt to account for the seemingly variable systemic velocity from night to night, but only did a single sine fit to both nights.

3.3 Doppler Maps

We used Doppler tomography on the most prominent emission lines in order to probe the structure of the accretion disk (Marsh & Horne 1988). In order to create the maps, we used the orbital period of 8.16 ± 0.02 hrs as determined by Callanan et al. (1990) and a systemic velocity derived from the radial velocity curve in Sect. 3.2. To comply with the standard definition of orbital phase 0 in Doppler maps (when the donor star is at inferior conjunction) we used the phasing derived from the Bowen map (see below) and applied a shift of $\simeq 0.5$ orbital phase compared to the value derived in Sect. 3.2.

Since He II $\lambda 4686$ is by far the strongest emission line in LMC X-2 we decided to create Doppler maps for each individual night, and we show the result in Fig. 4. Both maps show a ring-like structure, but there are some minor differences. During the second night it appears as if the outer edge of the structure is at higher velocities than during the first night ($218 \pm 10 \text{ km s}^{-1}$ compared to $180 \pm 10 \text{ km s}^{-1}$). Furthermore, during the first night there is a clear emission feature in the lower part of the map, that appears to have shifted toward the lower-right quadrant during the second night. Since we only have 2 nights of observations, it is not clear if these changes are real, but it suggests that there is some change in accretion disk structure from night to night.

We also created a Doppler map of the Bowen region by simultaneous fitting all the major N III ($\lambda 4634/4640$) and C III ($\lambda 4647/4650$) lines using the relative strengths as given by McClintock et al. (1975). The map is dominated by a bright emission feature, that we used to rotate the map (by $\simeq 0.5$ orbital phase) until it was located in the top. Fig. 5 shows the resulting map. The bright emission feature is at a velocity of $K_{\text{em}} = 351 \pm 28 \text{ km s}^{-1}$, and another (much fainter)

spot is also present in the map. If we interpret the bright spot as arising on the surface of the donor star (see Sect. 4.2), the fainter spot is in a region where we could expect an interaction between the accretion disk and the accretion flow. We do note that the velocity of the bright spot is much higher than the disk velocities in the HeII Doppler map (Fig. 4), and we will discuss this in Sect. 4.2. Furthermore, since the radial velocity curve in Sect. 3.2 could not exclude a 0.45 days orbital period, we also created a Bowen map for this period. Although there are several spots present in this map, none is as sharp and significant as those in Fig. 5. This is further support that the 0.32 day period is the correct orbital period.

4 DISCUSSION

4.1 Orbital period and the accretion disk

We have presented phase-resolved spectroscopy of LMC X-2, one of the brightest X-ray sources in the Large Magellanic Cloud, and also one of the most luminous LMXBs known. This enables us to derive the first constraints on its system parameters, and in particular give new insights on the previously reported orbital periods that ranged from $\simeq 6$ -8 hrs by Motch et al. (1985) or Callanan et al. (1990) up to $\simeq 12$ days by Crampton et al. (1990).

Callanan et al. (1990) based their claim of a short orbital period on an extended $\simeq 2$ week photometric campaign. A clear 8.15 hr modulation was present in their data that was interpreted as the orbital period, although there is indication of a long term ($\simeq 10$ day) variability that was also observed by Crampton et al. (1990). On the other hand, Crampton et al. did not detect the $\simeq 8$ hr period in a $\simeq 1$ week photometric campaign. However, there was a variation in the HeII radial velocity curve over a period of 4 nights in their spectroscopic data that they interpreted as a $\simeq 12$ day orbital period. Interestingly, they noticed that the H β emission lines also changed in strength over those 4 nights (even going into absorption), with maximum line strength occurring at minimum (continuum) light. Although Crampton et al. (1990) did speculate that the $\simeq 12$ day period is a precession or beat period, they discarded this due to the absence of shorter periods in their data set.

In Sect. 3.2 we have shown that there is a $\simeq 8$ hr period present in the radial velocity of HeII $\lambda 4686$ that is similar to the period detected by Callanan et al. (1990). Since the semi-amplitude of this radial velocity curve is rather small ($\simeq 41$ km s $^{-1}$), it might have been difficult to detect with the 4 m class telescope and an instrument with a resolution of ~ 4 Å used by Crampton et al. (1990). We, therefore, tentatively identify this period with the orbital period. However, that does leave the question of the long term variation observed by both Crampton et al. (1990) and Callanan et al. (1990). Similarly to Crampton et al. (1990), we also observe a large change in the emission line strength of H β , with a stronger line occurring at lower continuum flux levels. Unfortunately we only have two nights of observations, and are therefore not able to check if there is also a long term variation in our HeII radial velocity curve. However, Fig. 3 does suggest that during the second night (when the continuum flux was lower) either the amplitude or the mean velocity of the radial

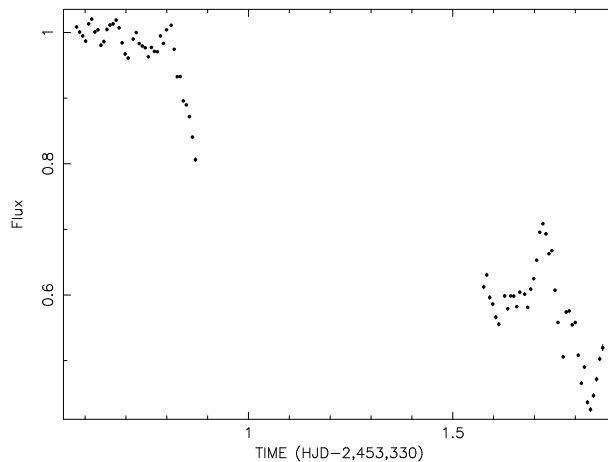


Figure 2. Lightcurve of the continuum light of LMC X-2 where the first night is normalised to unity.

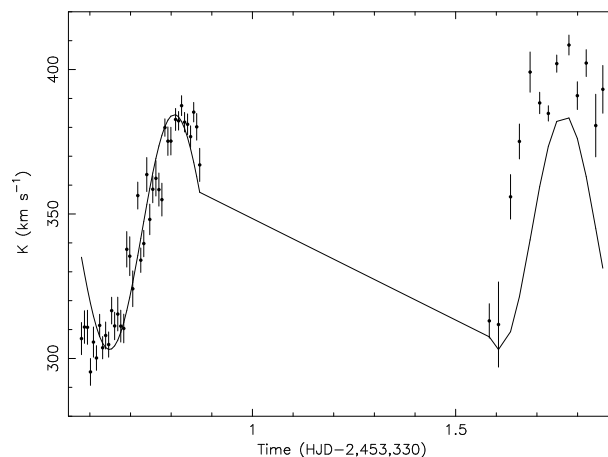


Figure 3. Best fit radial velocity curve derived from the core of the He II $\lambda 4686$ emission line.

velocity has increased compared to the first night (when the continuum flux was higher), similar to what Crampton et al. observed.

One explanation for the observed properties could be the presence of an inclined precessing, warped, accretion disk in LMC X-2, as is also observed in Hercules X-1 and SS 433 (Katz 1973, Margon 1984). We will discuss this suggestion in detail in a forthcoming paper by Shih et al. (in preparation), but here we will briefly highlight the spectroscopic evidence. During the first night we could be observing the accretion disk more edge on compared to the second night, and this could explain the much lower H β and HeI line intensities observed. This is further strengthened by the fact that the Doppler maps suggest that HeII is extending to higher radial velocities during the second night. If true, this could also explain the change in continuum flux observed in Fig. 2. Callanan et al. (1990) already suggested that a significant contribution to the optical light is either coming from the heated surface of the secondary or the outer disk bulge. If the fraction of the secondary or disk bulge that is in the shadow of the accretion disk changes as a function of precession period, this would lead to a change in the optical, with

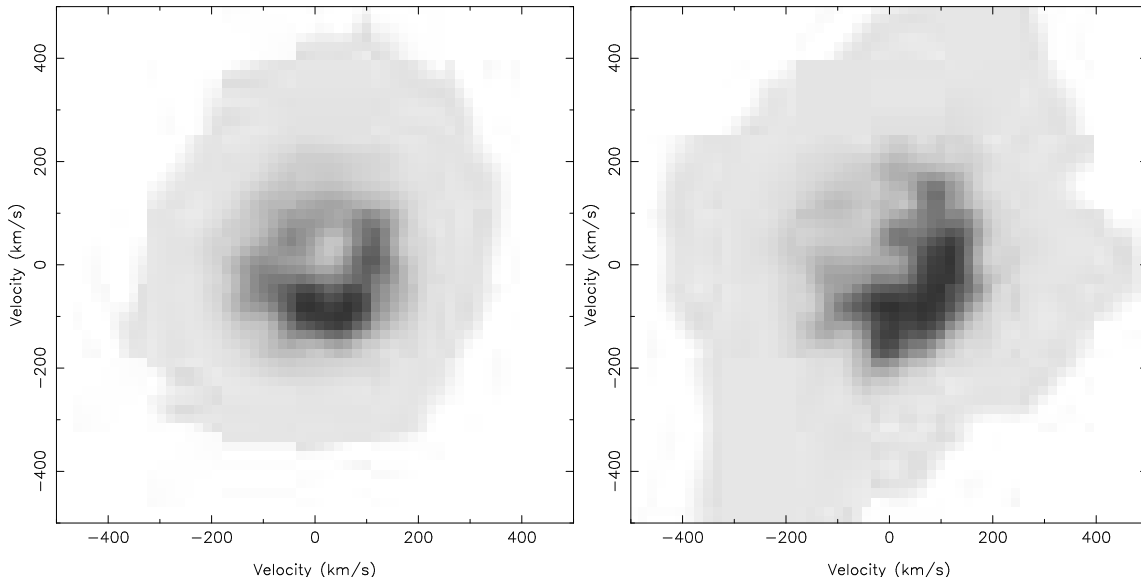


Figure 4. Doppler maps of the He II $\lambda 4686$ emission line in LMC X-2 for the first night of observations (left) and the second night (right).

maximum light occurring when the accretion disk is most edge on.

We can compare the characteristics of LMC X-2 to those of XTE J1118+480, an X-ray transient that is known for having a precessing (although not necessarily inclined) accretion disk (Uemura et al. 2000). Zurita et al. (2002) showed that the nightly average H α lines changed in both velocity and width that is consistent with a periodic variation on the precession period (Torres et al. 2004). Estimating the average wavelength of He II $\lambda 4686$ for the two nights in LMC X-2 gives 4690.37 ± 0.01 and 4690.70 ± 0.01 Å, respectively, suggesting a slight velocity shift. However, we must be careful with this slight shift, since we do not have a full orbital coverage each night and this could lead to a systematic off-set to the average wavelength. A better way to find out if this slight shift in velocity is real, is by examining the two He II Doppler maps. They show a bright spot that appears to have moved over night, suggesting the presence of an irradiated region that shows movement on a much longer time-scale than the orbital period, such as the warped and irradiated part of the accretion disk. Unfortunately, we only have two nights of data and can therefore not follow the long-term evolution of this bright spot to unambiguously claim that it moves periodically on a longer timescale. A spectroscopic campaign with a VLT-class telescope would be needed to follow the evolution of the emission lines in LMC X-2 over a full expected precession cycle (of $\simeq 1$ week) and show that this bright spot in the He II Doppler maps is long-lived and connected to a precessing disk.

4.2 K-velocities?

The radial velocity curve of the He II $\lambda 4686$ emission line shows a periodic variability that we have interpreted as the orbital period. This could suggest that it also traces the primary and that we have an estimate for both orbital phase zero and K_1 . However, the Doppler maps in Fig. 4 show that the He II emission is dominated by the bright spot due to

the warped accretion disk. Since this spot does not have a similar phasing as the primary (and even moves due to precession), we cannot use the radial velocity curve to determine the orbital phasing of the primary. Furthermore, if LMC X-2 harbours an inclined precessing accretion disk it is also not likely that semi-amplitude of the He II radial velocity curve traces K_1 . In this case the accretion disk, or at least the irradiated side that produced the bright spot in the He II Doppler map, is tilted out of the orbital plane thereby changing its radial velocity. This is clear from Fig. 3, where it appears that either the average velocity or the semi-amplitude of the radial velocity curve has changed. Only from long-term spectroscopic monitoring of LMC X-2 might it be possible to determine the K_1 velocity, but currently we cannot constrain this value. This also means that currently we cannot be certain that the average velocity that we determined corresponds to the systemic velocity γ .

We have detected narrow emission lines in the Bowen region that dominate the Bowen Doppler map. Although these lines are not visible in the individual spectra, they become prominent when we create an average spectrum that is shifted into the rest-frame of these narrow lines. As Fig. 6 shows, all important Bowen lines are present, and especially the N III $\lambda 4640$ line is very strong, suggesting that this spot is real and not just a noise feature in the Doppler map. These narrow lines have been detected in many other X-ray binaries thus far, such as Sco X-1, X 1822–371, GX 339–4, V801 Ara, V926 Sco, Aql X-1, GX 9+9 and GR Mus (Steeeghs & Casares 2002, Casares et al. 2003, Hynes et al. 2003, Casares et al. 2006, Cornelisse et al. 2007a,b, Barnes et al. 2007). Since there are few compact regions that could produce such narrow emission lines, it was proposed that they arise on the irradiated surface of the donor star. Especially in X 1822–371, but also in V801 Ara this connection could unambiguously be made, strengthening the claim in all other sources. Furthermore, the width of these emission lines in LMC X-2 suggests that they come from a very compact region in the system, and apart from the donor star surface not

many other regions in the binary could produce such narrow lines. Therefore, following the other systems and given the narrowness of these emission lines we tentatively identify them as coming from the donor star of LMC X-2, despite the fact that the absolute phasing of the system is unknown.

In LMC X-2 there is another problem with identifying the compact spot in the Bowen Doppler map with the secondary, namely the fact that all emission in the He II Doppler maps is at much lower velocities than the compact Bowen spot. This would suggest that all emission in the He II map is at sub-Keplerian velocities, and not related to the accretion disk. However, such behaviour is not unique to LMC X-2. Also in the He II $\lambda 4686$ Doppler maps of many other LMXBs (such as Sco X-1, X 1822–371, V801 Ara and V926 Sco amongst others) is most, if not all, emission at sub-Keplerian velocities (Steehgs & Casares 2002, Casares et al. 2003, 2006). However, if the compact spot in the Bowen map is produced on the donor star, LMC X-2 would be the most extreme system in showing too low disk velocities. We do note that one of the assumptions of the technique of Doppler tomography is that all motion occurs in the orbital plane. If the accretion disk in LMC X-2 is inclined, as suggested above, these assumptions are no longer fulfilled. This would make the interpretation of the accretion disk structure using the Doppler maps more difficult, and could be a reason why we observe these sub-Keplerian velocities. For example, in SS 433 the precession angle of the jets (and most likely also the accretion disk) is thought to be $\simeq 20^\circ$ (Margon 1984), and if LMC X-2 has a similar precession angle (and a relatively low inclination) this could easily account for observed accretion disk velocities that are a factor 2 too low. Again, long term spectroscopic monitoring would be needed to give more insight into the real accretion disk velocities. However, we do note that this should not impact our interpretation of the compact spot arising on the secondary star, and we remain confident that we have detected a signature of the donor star.

4.3 System parameters

Assuming that we have detected the donor star in LMC X-2 we can use these data to constrain the system parameters. Firstly, the narrow lines must arise on the irradiated surface, therefore the determined K_{em} ($351 \pm 28 \text{ km s}^{-1}$) must be a lower limit to the center of mass velocity of the secondary (K_2). However, since K_{em} must be smaller than K_2 this already gives a lower limit to the mass function of $f(M) = M_1 \sin^3 i / (1+q)^2 \geq 0.86 M_\odot$ (at 95% confidence), where q is the binary mass ratio M_2/M_1 and i the inclination of the system. In order to further constrain the mass function the K -correction must be determined. Unfortunately, this depends on q , i and the disk flaring angle α , all of which are unknown for LMC X-2 (Muñoz-Darias et al. 2005). Furthermore, the K -correction by Muñoz-Darias et al. (2005) assumes an idealised accretion disk that is located in the orbital plane of the system, both of which are most likely not true for LMC X-2. Therefore, we must be very careful with any constraints we will derive in the rest of this section.

We can set a strict lower-limit to K_2 by assuming that it is equal to K_{em} , i.e that all emission is coming from the poles. Furthermore, we can use the 4th order polynomials for the K -correction by Muñoz-Darias et al. (2005) to determine

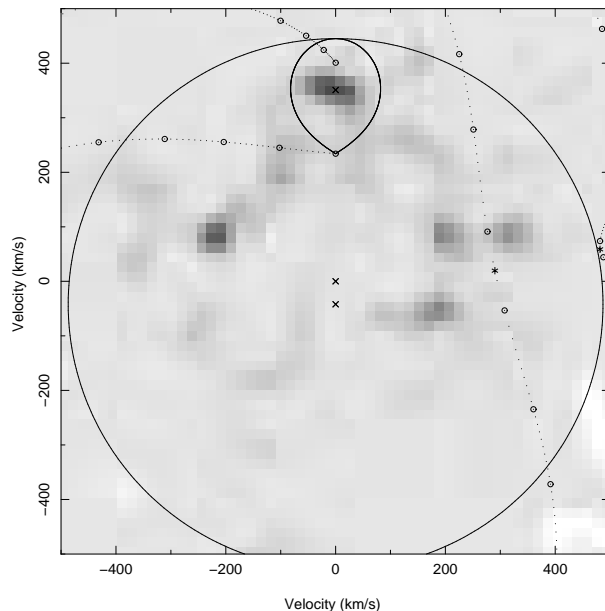


Figure 5. Doppler map of the Bowen region in LMC X-2. The constrained spot in the top of the diagram is at a position where a donor star signature is expected. Superposed are the Roche-lobe, gas stream leaving the L1 point, and the Keplerian velocity along the stream for a random set of allowed parameters ($q=0.12$ and $K_2=351 \text{ km s}^{-1}$). The circle indicates the Keplerian velocity at the outer edge of the accretion disk.

K_2 as a function of q in the case of $\alpha=0^\circ$ and $i=40^\circ$ (since LMC X-2 does not show dips or eclipses its inclination must be lower than $\simeq 70^\circ$, and therefore the polynomials for the K -correction when $i=40^\circ$ are a better approximation than in the case of $i=90^\circ$). We show these limits on K_2 in Fig. 7. Note that these limits are still true even if the accretion disk is severely warped or out of the orbital plane.

Assuming that the width of the narrow emission lines is mainly due to rotational broadening we can derive a lower-limit to q using $V_{\text{rot}} \sin i = 0.462 K_2 q^{1/3} (1+q)^{2/3}$ (Wade & Horne 1988). From Fig. 6 we derive a $FWHM$ of the narrow lines of $90.2 \pm 18.8 \text{ km s}^{-1}$. Since these emission lines are expected to arise from only part of the secondary, this value must be a strict lower-limit and the true $FWHM$ must be higher. Furthermore, our estimate still includes the effect of the intrinsic instrumental resolution of 70 km s^{-1} . Following Casares et al. (2006) we accounted for this effect by broadening a strong line in our arc spectrum using a Gray rotational profile without limb darkening (since the fluorescence lines occur in optically thin conditions) until we reached the observed $FWHM$ (Gray 1992). We found that a rotational broadening of $V_{\text{rot}} \sin i \geq 60 \pm 18 \text{ km s}^{-1}$ reproduced our results. Since this is a strict lower-limit on the true rotational broadening this will also give a lower limit on both q and K_2 that is shown in Fig. 7.

Casares et al. (2006) derived an upper-limit to q by assuming that the secondary is the largest possible zero-age main sequence star fitting in its Roche-lobe. However, LMC X-2 shows the X-ray properties of a Z-source (Smale et al. 2003). Z-sources trace a Z-like shape in their X-ray colour-colour diagrams and are thought to have more evolved secondaries (see e.g. Hasinger & van der Klis 1989).

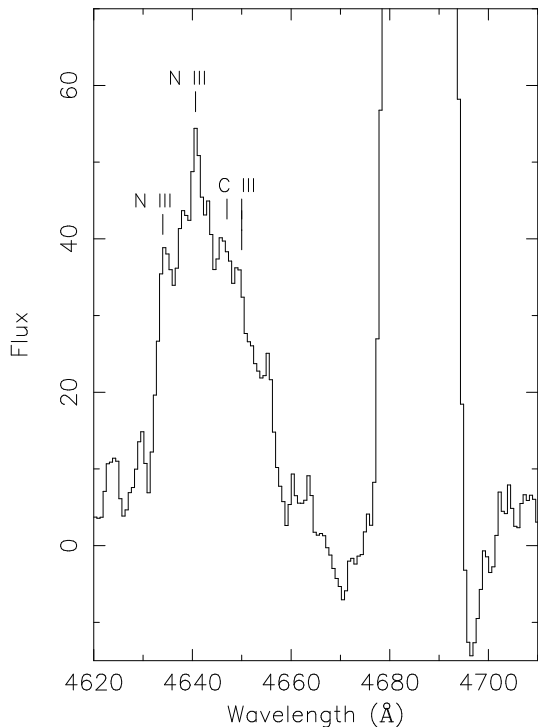


Figure 6. Average spectrum of the Bowen region in the rest-frame of the narrow emission lines in LMC X-2. We have indicated the main lines in this region.

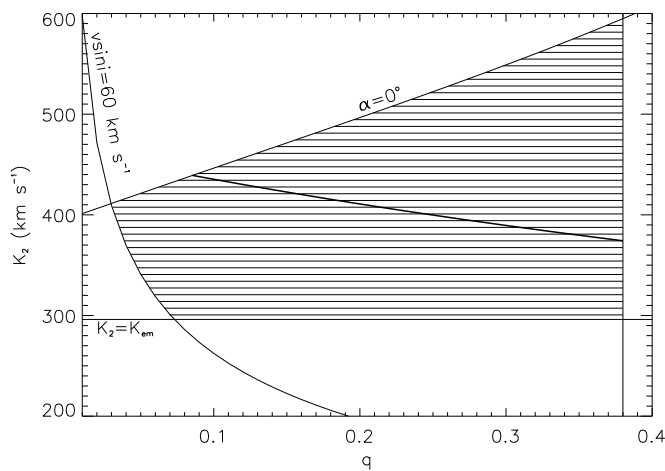


Figure 7. Constraints on q and K_2 for LMC X-2 indicated by the shaded area. K_2 must be larger than K_{em} , while the disk flaring angle must be larger than $\alpha=0^\circ$. Rotational broadening of the narrow lines gives the lower constraints on q while the assumption that the accretion disk is precessing gives the upper-limit. The solid dark line drawn through the shaded area indicates where $M_1 \sin^3 i = 3.2 M_\odot$; above this line the compact object must be a black hole.

Although the evolved nature of the secondary in Z-sources is not unambiguously confirmed, it is still reasonable that the assumption of a zero-age main sequence donor is most likely not true for LMC X-2. We therefore cannot use this assumption to derive an upper-limit on the mass ratio, since the evolved donor star could be more massive than a main se-

quence star (Schenker & King 2002). However, we can use an alternative way to set an upper-limit to q , namely using the fact that LMC X-2 has a precessing accretion disk. One of the main criteria to produce a precessing accretion disk is to have an extreme mass ratio (e.g. Whitehurst 1988). From an overview by Patterson et al. (2005) of compact binaries that have a precessing accretion disk and for which the mass ratio is known, we can use the system with the largest measured q thus far and assume that it must be smaller for LMC X-2. This leads to a conservative upper-limit of $q \leq 0.38$, and our final limit for the system parameters shown in Fig. 7. All these limits constrain an area in Fig. 7 that is still quite large, and at the moment it is still not possible to constrain any of the system parameters tightly enough in order to say anything about the component masses or the evolution of LMC X-2. However, we can make two more assumptions, although more speculative, for LMC X-2 to further constrain its system parameters.

Given that LMC X-2 shows the X-ray properties of a Z-source (Smale et al. 2003), we can speculate that its compact object is a neutron star. In this case the maximum mass for the compact object would be $\simeq 3.2 M_\odot$, and we could use this to set tighter upper-limits to K_2 than derived from the assumptions we have made thus far. In Fig. 7 we have therefore also indicated the maximum limit where the compact object can still be a neutron star, i.e. where $M_1 \sin^3 i = 3.2 M_\odot$, as a solid dark line. However since we cannot completely rule out the possibility that the compact object in LMC X-2 is a low mass black hole, we have decided not to use this limit to constrain K_2 . Finally, we can speculate that the semi-amplitude that we have derived from the He II $\lambda 4686$ radial velocity curve is K_1 . In this case we set an upper-limit to $q = K_1 / K_{em} \leq 0.12$. Note that we have used this value for q and $K_2 = K_{em}$ to draw the Roche lobe in Fig. 5 to illustrate that it encompasses the bright spot. However, this set of system parameters is just one possible solution within the allowed region in Fig. 7 and we do not imply that it represents the true or even preferred system parameters of LMC X-2.

We note that this value of $q = 0.12$ is similar to the mass ratios determined from other X-ray binaries that show a precessing accretion disk (O’Donoghue & Charles 1996), suggesting that it might be close to the true mass ratio of LMC X-2. Also, if we assume that the $\simeq 12$ day variation observed by Crampton et al. (1990) is the precession period, and that the 8.2 hr photometric period is a superhump period, we can estimate the fractional period excess of the superhump over the orbital period ϵ . We find that $\epsilon \simeq 0.03$ and with the $\epsilon(q)$ - q relation by Patterson et al. (2005) we estimate that $q \simeq 0.14$. This is again close to the mass ratio derived above. Although this would set tight constraints to q , and makes a black hole nature for the compact object very unlikely, we have argued in Sect. 4.2 that we cannot make this assumption and have therefore not plotted this in Fig. 7.

Finally, we do want to point out that, despite the large range of system parameters possible, LMC X-2 most likely harbours a neutron star that is more massive than the canonical $1.4 M_\odot$. Since LMC X-2 does not show eclipses or dips we can estimate an upper-limit on the inclination of 65° (see e.g. Paczynski 1974). Combined with the lower limit on the mass function already gives $f(M_1) / \sin^3 i \geq 1.16 M_\odot$. For the compact object to be $1.4 M_\odot$, this only leaves $q \leq 0.10$

(and $M_2 \leq 0.14$). Furthermore, already for $K_2 = 309 \text{ km s}^{-1}$ (and $i \leq 65^\circ$) the mass of the compact object will exceed $1.4 M_\odot$. This only leaves a very small corner in the bottom-left part of our allowed system parameters, and makes LMC X-2 another strong candidate to harbour a massive neutron star.

5 CONCLUSIONS

We have detected for the first time a spectroscopic period in LMC X-2 that is close to previously published photometric period of 8.15 hrs by Callanan et al. (1990). We interpret this as the orbital period, while the 12 day period detected by Crampton et al. (1990) is most likely the super-orbital period due to an inclined precessing accretion disk. The signature of such a precessing accretion disk is also present in our data, mainly in the He II Doppler maps, but also in the form of a nightly change in semi-amplitude and/or mean velocity of the radial velocity curve of He II $\lambda 4686$. In a forthcoming paper by Shih et al. (in prep.) we will explore the consequences of such a precessing accretion disk in more detail.

The main result of our spectroscopic data-set is the detection of narrow emission lines in the Bowen region. Following previous detections of such lines in other LMXBs, we tentatively identify these as arising from the surface of the secondary. This gives us for the first time the possibility to derive the mass function of LMC X-2 and constrain its system parameters. Although they point toward a massive neutron star, the constraints on the system parameters are currently not very tight. However, this could change with a better determination of both the spectroscopic and precession period during a long term spectroscopic campaign to study the emission line kinematics. Using the relation between the mass ratio q and the fractional period excess of the spectroscopic and the photometric period ϵ could give strong constraints on q and thereby the other system parameters. In particular this would be an excellent way to identify the nature of the donor star to find out if Z-sources really have more evolved secondaries.

ACKNOWLEDGEMENTS

This work is based on data collected at the European Southern Observatory Paranal, Chile (Obs.Id. 074.D-0657(A)). We acknowledge the use of the MOLLY and DOPPLER software packages developed by T.R. Marsh. RC acknowledges financial support from a European Union Marie Curie Intra-European Fellowship (MEIFT-CT-2005-024685). JC acknowledges support from the Spanish Ministry of Science and Technology through project AYA2002-03570. DS acknowledges a Smithsonian Astrophysical Observatory Clay fellowship as well as support from NASA through its Guest Observer program. DS acknowledges a PPARC/STFC Advanced Fellowship.

REFERENCES

- Alcock, C., Allsman, R.A., Alves, D.R., Axelrod, T.S., Becker, A.C., Bennett, D.P., Charles, P.A., Cook, K.H., Drake, A.J., Freeman, K.C., and 16 coauthors 2000, MNRAS; 316, 729
- Barnes, A.D., Casares, J., Cornelisse, R., Charles, P.A., Steeghs, D., Hynes, R.I., O'Brien, K. 2007, MNRAS, accepted for publication [astro-ph/0707.0624]
- Casares J., Steeghs D., Hynes R.I., Charles P.A., O'Brien K., 2003, ApJ, 590, 1041
- Casares, J., Cornelisse, R., Steeghs, D., Charles, P.A., Hynes, R.I., O'Brien, K.O., & Strohmayer, T.E. 2006, MNRAS, 373, 1235
- Cornelisse, R., Casares, J., Steeghs, D., Barnes, A.D., Charles, P.A., Hynes, R.I., O'Brien, K. 2007a, MNRAS, 375, 1463
- Cornelisse, R., Steeghs, D., Casares, J., Charles, P.A., Barnes, A.D., Hynes, R.I., O'Brien, K. 2007b, MNRAS, accepted for publication [astro-ph/0707.0449]
- Callanan, P.J., Charles, P.A., van Paradijs, J., van der Klis, M., Pedersen, H., Harlaftis, E.T. 1990, A&A, 240, 346
- Crampton, D., Hutchings, J.B., Cowley, A.P., Schmidtke, P.C., Thompson, I.B. 1990, ApJ, 355, 496
- Hynes, R.I., O'Brien, K. 2007, MNRAS, 375, 1463
- Hasinger, G., & van der Klis, M. 1989, A&A, 225, 79
- Gray, D.F., 1992, "The Observation and Analysis of Stellar Photospheres", CUP, 20
- Horne K., 1986, PASP, 98, 609
- Hynes R.I., Steeghs D., Casares J., Charles P.A., O'Brien K., 2003, ApJ, 583, L95
- Katz, J.I. 1973, Nature, 246, 87
- Margon, B. 1984, ARA&A, 22, 507
- Marsh T.R., Horne K., 1988, MNRAS 235, 269
- McClintock, J.E., Canizares, C.R., & Tarter, C.B. 1975, ApJ, 198, 641
- Motch, C., Chevalier, C., Ilovaisky, S.A., Pakull, M.W. 1985, Space Sci. Reviews, vol. 40, p. 239
- Motch, C., Pakull, M.W. 1989, A&A, 214, L1
- Muñoz-Darias, T., Casares, J., & Martínez-Pais, I.G. 2005, ApJ, 635, 502
- O'Donoghue, D., Charles, P.A. 1996, MNRAS; 282, 191
- Paczynski, B. 1974, A&A, 34, 161
- Pakull, M. 1978, IAU Circ., 3313
- Patterson, J., Kemp, J., Harvey, D.A., Fried, R.E., Rea, R., Monard, B., Cook, L.M., Skillman, D.R., Vanmunster, T., Bolt, G., et al. 2005, PASP; 117, 1204
- Scargle, J.D. 1982, ApJ, 263, 835
- Schenker, K., King, A.R. 2002, ASP Conf.Ser. 261, "The Physics of Cataclysmic Variables and Related Objects", 261, 242
- Steeghs D., Casares J., 2002, ApJ, 568, 273
- Smale, A.P., Kuulkers, E. 2000, ApJ, 528, 702
- Smale, A.P., Homan, J., Kuulkers, E. 2003, ApJ, 590, 1035
- Torres, M.A.P., Callanan, P.J., Garcia, M.R., Zhao, P., Laylock, S., Kong, A.K.H. 2004, ApJ, 612, 1026
- Uemura, M., Kato, T., Matsumoto, K., Honkawa, M., Cook, L., Martin, B., Masi, G., Oksanen, A., Moilanen, M., Novak, R., Sano, Y., Ueda, Y. 2000, IAUC, 7418
- Wade R.A., Horne K., 1988, ApJ, 324, 411
- Whitehurst, R. 1988, MNRAS, 232, 35
- Zurita, C., Casares, J., Shahbaz, T., Wagner, R.M., Foltz, C.B., Rodriguez-Gil, P., Hynes, R.I., Charles, P.A., Ryan, E., Schwarz, G., & Starrfield, S.G. 2002, MNRAS, 333, 791

This paper has been typeset from a \TeX / \LaTeX file prepared by the author.